Australian Institute of Nuclear Science and Engineering and by the Research Committee of the University of Western Australia. One of us (AC) gratefully acknowledges receipt of the University Research Studentship.

References

BOATNER, L. A. & ABRAHAM, M. M. (1967). *Phys. Rev.* **163**, 213–219.
BOWDEN, C. M. (1966). *Bull. Am. Phys. Soc.* **11**, 834.
BOWDEN, C. M. (1967). Doctoral Dissertation, Clemson Univ., South Carolina, USA.
CHATTERJEE, A., MASLEN, E. N. & WATSON, K. J. (1988). *Acta Cryst.* B**44**, 381–386.
COWAN, R. D. (1973). *Nucl. Instrum. Methods*, **110**, 173–182.
DUNITZ, J. D., SCHWEIZER, W. B. & SEILER, P. (1983). *Helv. Chim. Acta*, **66**, 123–133.
FUJINO, K., SASAKI, S., TAKEUCHI, Y. & SADANAGA, R. (1981). *Acta Cryst.* B**37**, 513–518.
IWATA, M. & SAITO, Y. (1973). *Acta Cryst.* B**29**, 822–832.
MARUMO, F., ISOBE, M. & AKIMOTO, S. (1977). *Acta Cryst.* B**33**, 713–716.
MARUMO, F., ISOBE, M., SAITO, Y., YAGI, T. & AKIMOTO, S. (1974). *Acta Cryst.* B**30**, 1904–1906.
SASAKI, S., FUJINO, K. & TAKEUCHI, Y. (1979). *Proc. Jpn Acad. Ser. B*, **55**, 43–48.
SHINTANI, H., SATO, S. & SAITO, Y. (1975). *Acta Cryst.* B**31**, 1981–1982.
SPACKMAN, M. A. & MASLEN, E. N. (1985). *Acta Cryst.* A**41**, 347–353.
VARGHESE, J. N. & MASLEN, E. N. (1985). *Acta Cryst.* B**41**, 184–190.

Acta Cryst. (1988). B**44**, 395–406

Crystallography of Systems with Long Periods: a Neutron-Scattering Study of Sodium Dodecyl Sulfate/Water Mesophases

BY P. KÉKICHEFF

Laboratoire de Physique des Solides, associé au CNRS (LA 2), Bâtiment 510, Université de Paris-Sud, 91405 Orsay, France

AND B. CABANE

DPC–SCM–UA 331, CEN Saclay, 91191 Gif-sur-Yvette, France

(*Received 7 July* 1987; *accepted 7 March* 1988)

Abstract

Diffraction patterns are presented for the ordered mesophases of the sodium dodecyl sulfate (SDS)/water lyotropic system. The reciprocal space of the six mesophases has been determined directly through the use of oriented samples. It changes in a nearly continuous way from the most hydrated phase (hexagonal: circular cylinders) to the least hydrated phase (lamellar: bilayers). The orientational behavior of these oriented mesophases has also been used to identify their leading crystallographic planes; this yields an approximate representation of real-space structures. Accordingly, the path from the homogeneously curved cylindrical phase to the flat lamellar phase goes through the production of structures with inhomogeneously curved interfaces (ribbons) or with negative Gaussian curvature (saddle-splay geometry).

1. Introduction

Crystalline arrays of interfaces are formed when amphiphilic molecules (soaps, salts of long chain acids, or other surfactants) are mixed with water in adequate proportions (Ekwall, 1975; Winsor, 1968). These mixtures are liquids because the amphiphilic molecules are in a liquid state, as shown by their wide-angle scattering, where the interferences between neighboring amphiphilic chains show up as a diffuse ring (Luzzati, 1968). These mixtures are also crystals because the array of interfaces is periodic in one, two or three dimensions, as shown by the small-angle scattering where the repetition of interfaces produces sharp diffraction lines (Luzzati, 1968).

The shapes of such interfaces are governed by a set of constraints at the molecular level (Charvolin & Tardieu, 1978). On the one hand, the segregation of polar and apolar groups requires that the separations between interfaces should be of the order of the length of an amphiphilic molecule. On the other hand, the effective forces between the hydrated polar heads (electrical repulsions) and those between the lipidic aliphatic chains (oil–water surface tension) tend to impose a certain value for the curvature of the interfaces. This 'desired' curvature may not be compatible with a radius which is of the order of a molecular length: this is the basic problem behind the shapes of interfaces which has been analyzed in terms

0108-7681/88/040395-12$03.00

of frustration (Sadoc & Charvolin, 1986; Charvolin & Sadoc, 1987).

The traditional view has been that in this situation amphiphilic systems will separate into a phase where the interfaces have a high curvature (radius of the order of the molecular length) and a phase of zero curvature. More recently it has been recognized that the conflict can be resolved either through negative Gaussian curvature or through inhomogeneous curvatures (Hendrikx & Charvolin, 1981; Alpérine, Hendrikx & Charvolin, 1985). The picture is also complicated by the interactions between successive interfaces: these forces set the optimum distance between interfaces and determine their mode of packing.

In previous work, we used X-ray diffraction to study the transition from a situation with homogeneously curved interfaces (cylinders) to one with zero curvature (bilayers) in the system SDS/water, where SDS stands for sodium dodecyl sulfate (Kékicheff & Cabane, 1987). Powder diffraction spectra show that this process occurs through the production of four intermediate mesophases between the cylindrical and the lamellar mesophases; some of these mesophases show obvious relations to each other, suggesting that the whole transition might be nearly continuous. However to describe the structures and understand the physical reasons for the phase changes, the shapes of the amphiphilic aggregates and their relative locations must be determined. So far, we have not been able to obtain this information directly from the relative intensities of the diffraction lines, because the signs of the diffracted amplitudes were not known to us; indeed for X-rays the form factor of SDS aggregates is not simple, as polar heads and aliphatic tails have scattering densities on either side of water and minor errors in these densities can alter the phases of the diffraction lines.

In the present work, we continue the study of the structures of these mesophases: the use of oriented samples and that of high fluxes of neutrons allows us to confirm the previous structures, and to extract some information about the shapes of the aggregates. At our level of resolution, we observe that the geometry of the aggregates changes nearly continuously from the most hydrated mesophase (two-dimensional hexagonal array of infinite cylinders) to the least hydrated one (one-dimensional packing of flat bilayers). At temperatures between 325 and 360 K, the changes occur through a deformation of the cylinders (hexagonal phase 'H_α') into ribbons (two-dimensional monoclinic phase 'M_α'), which then merge two by two sideways (period doubling) and also at regular intervals along their length (three-dimensional rhombohedral phase 'R_α'). A continuous deformation of this phase leads to an optically isotropic phase (cubic phase 'Q_α'); then the cubic phase is stratified into separate layers which are piled in a staggered configuration (three-dimensional tetragonal phase 'T_α'). Finally the correlations between these layers are lost, yielding a lamellar phase 'L_α', whose layers still contain a collection of defects with the short-range correlations of the tetragonal phase.

2. Methods

2.1. *Materials*

The amphiphile used in this work is sodium dodecyl sulfate (SDS); it was purchased from British Drug Houses (grade 'specially pure'), reneutralized to remove acid impurities (Kékicheff, Cabane & Rawiso, 1984*a*), and dried at 338 K in a vacuum for 48 h. This procedure ensures good stability of the mesophases for a few days at 338 K. For neutron scattering, the mesophases were made with D_2O (99·99% isotopically pure from ORIS–BIS) in order to obtain a good contrast between the polar and apolar regions. The procedures used for preparing the mesophases and assessing their homogeneity are identical to those previously described (Kékicheff & Cabane, 1987; Kékicheff, Cabane & Rawiso, 1984*a*).

2.2. *Samples*

For the study of mesophases, the main advantage of neutrons over X-rays is that thick samples can be used; such samples can be oriented through surface alignment, and observed with the beam parallel or normal to the direction of alignment. Our samples were prepared by pushing a mesophase into a stack of 40 thin quartz plates, with regular spacings of 50 μm between the plates; the flow of the mesophase through the stack produced an orientation of its aggregates parallel to the plates; this orientation was maintained by anchoring of the SDS molecules on the plates. The whole stack was contained in a fluorimeter quartz cell, which was placed in an aluminium cell with quartz windows. The escape of water vapour from the sample was prevented by a buffer of excess sample in the quartz cell, and then by 'O' rings closing the aluminium cells. This design was in general quite satisfactory: the quality of the results was completely determined by the type of alignment obtained for the mesophase.

2.3. *Control of neutron beams and data collection*

The neutron-scattering experiments were performed at the Institute Laüe–Langevin (ILL) in Grenoble on the instrument D17 ($\lambda = 10{\cdot}2$ Å; $\Delta\lambda/\lambda = 5\%$) and at the Laboratoire Léon Brillouin (LLB) in Saclay on the instrument PAXY ($\lambda = 4{\cdot}3$ Å; $\Delta\lambda/\lambda = 5\%$). This spread in wavelengths can be tolerated for oriented samples, because diffraction spots corresponding to similar Q-scattering vectors but different orientations in reciprocal space will be resolved. The data were collected on the two-dimensional xy detectors of both instruments and normalized by the incoherent scattering of water.

Two artifacts should be considered in the scattering of neutrons by such oriented samples. One is the specular reflexion of the neutrons at the interfaces between the quartz plates and the mesophase, in the geometry where the beam is nearly parallel to these plates. This reflexion will produce an intense stripe on the equator along the normal to the plates (Fig. 1). This pattern can be on either side of the beam depending on the particular angle of the plates to the beam; it can shadow some of the low-angle diffraction spots, in particular the one at $Q = 0{\cdot}07$ Å^{-1} for intermediate phases. The other is multiple scattering caused by the large thickness of the sample (5 mm); this could produce a diffuse stripe near the beam stop (Kékicheff, Cabane & Rawiso, 1984*b*; Hendrikx, Charvolin, Kékicheff & Roth, 1987) and also enhance the intensities of second-order diffraction lines (it is not an important effect for the intermediate mesophases studied here).

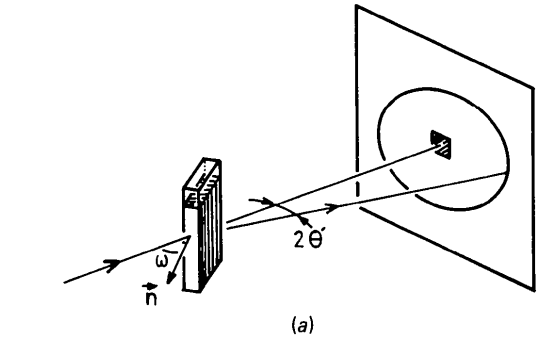

(*a*)

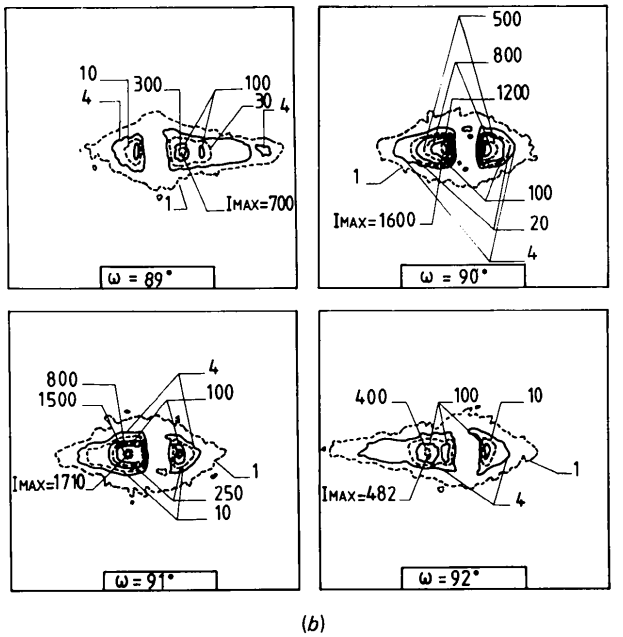

(*b*)

Fig. 1. (*a*) Scattering geometry for a cell containing a stack of 50 quartz plates in D_2O; ω is the tilt angle of the cell with respect to a situation where the plates are normal to the beam; 2θ is the scattering angle of the neutrons. (*b*) Specular reflexion of the neutrons at the interface between the quartz plates and D_2O: when the tilt angle ω is close to 90°, the condition for total reflexion is met, and the reflected neutrons produce an intense horizontal stripe on the detector. The figure shows contour maps of the diffraction pattern recorded on D17 (sample-to-detector distance: 3·46 m).

3. Results

The information presented in this paper is largely derived from an analysis of the way in which intermediate mesophases align along quartz plates, which allows their leading crystallographic planes to be identified. For this analysis it is necessary to understand the patterns of rings and spots which may be produced when two- or three-dimensional mesophases are aligned along flat plates: this is presented below.

3.1. *Crystalline phases*

The diffraction patterns of crystalline phases are instructive because they show the best alignment which can be obtained through our system of stacked thin layers; all the other experimental broadenings (besides misorientations within the sample) are revealed. Fig. 2 shows the diffraction pattern from a stack of slightly hydrated SDS crystals; here the layers are vertical, and the neutron beam is parallel to them. The scattered neutrons, collected on an *xy* detector, map a plane of the reciprocal space of the crystals; this plane contains the two first diffraction orders of the layers (periodicity $a = 37{\cdot}9$ Å).

3.2. *Hexagonal mesophase 'H_α'*

The reciprocal space of a hexagonal phase is a two-dimensional array of spots in the equatorial plane, normal to the long axes of the cylinders, also with hexagonal symmetry. If the sample contains many domains that share the same direction of orientation for the long axes of the cylinders but have different orientations of the array around the axis, then the hexagonal symmetry of the reciprocal space is lost: each diffraction spot describes a ring around this axis, and a set of concentric rings is obtained in the equatorial plane, with spacings in the ratios 1, $\sqrt{3}$, $\sqrt{4}$, $\sqrt{7}$, $\sqrt{9}$, ... If the long axes are also allowed to rotate, while remaining parallel to the quartz plates, then for each diffraction order, there will be a series of rings, which all meet along an equatorial line which is normal to the plates.

In a scattering experiment, where the beam is *parallel* to the quartz plates (Fig. 3), a section of the reciprocal space by a plane normal to the beam will be seen. This section will contain one set of the above mentioned rings, with the regular spacings 1, $\sqrt{3}$, $\sqrt{4}$, $\sqrt{7}$, $\sqrt{9}$, ... ; it will also contain the equator, where *all* rings meet; consequently, the scattering pattern will have

rings, with intense spots where these rings meet the equator. In a scattering experiment where the beam is *normal* to the plates (Fig. 4) a section of the reciprocal space by a plane parallel to the plates will be observed; this section is made of other rings, with the same spacings.

In fact, for the hexagonal phase H_α, the diffraction pattern which we observe with the beam parallel to the plates shows six spots on the first-order ring, located at the apexes of a regular hexagon, instead of just two spots located on the equator (Fig. 5*a*). These spots are produced by domains with their long axes along the beam; the hexagonal pattern implies that such domains take a special orientation along the plates instead of rotating freely along their long axes. Fig. 5(*b*) shows that this alignment allows the mesophase to build the set of densest reticular planes along the quartz plates. For these domains, the diffracted neutrons map a plane of reciprocal space which corresponds to the two-dimensional packing of the cylinders; it consists of a triangular array of spots, of which only the first-order ones are seen. The corresponding unit cell is defined by two vectors leaving the center of the beam and ending on two neighboring apexes of the hexagon. Its dimensions match those measured on the X-ray powder patterns, with a real space dimension of 47·4 Å at a water content of 50·2%.

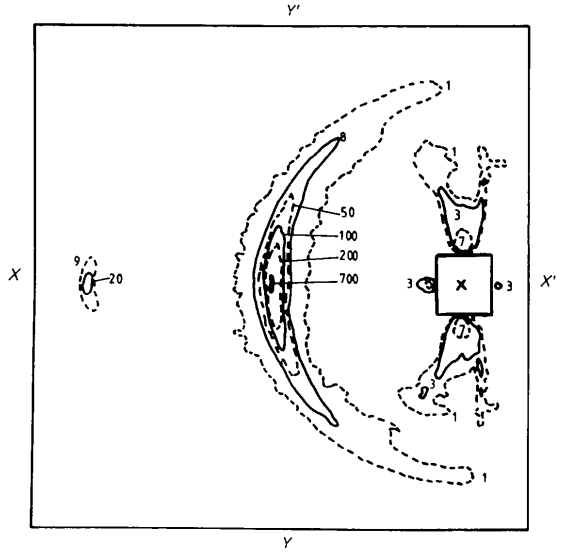

Fig. 2. Diffraction by crystals of solid SDS at low hydration. This solid has a lamellar structure; its bilayers are aligned by vertical quartz plates, and the neutron beam is parallel to the plates ($\omega = 90°$ in Fig. 1*a*). The horizontal axis of the pattern (equator) which is normal to the beam and to the plates, is also the symmetry axis of reciprocal space. The crescents which are centered on this axis are the first and second diffraction orders for the repetition of bilayers; their transverse width along the horizontal axis matches the wavelength dispersion of the beam (5%), while their elongation is caused by the disorientations of the layers (~2°). The scattering next to the beam on the equator is due to specular reflexion of neutrons by the quartz plates (Fig. 1*b*); the vertical crescents next to the beam are caused by double scattering on the first diffraction order.

3.3. *Intermediate mesophases*

These phases are located between the hexagonal H_α and lamellar L_α phases of the SDS/water system. We have demonstrated the existence of four intermediate mesophases, and have labeled them M_α, R_α, Q_α and T_α in order of increasing SDS concentrations (Kékicheff & Cabane, 1987). In a temperature concentration phase diagram (Fig. 6) their boundaries rise nearly vertically above a set of minimum temperatures, which are at about 315 K (Kékicheff, Grabielle-Madelmont & Ollivon, 1988).

3.3.1. *Two-dimensional monoclinic phase 'M_α'.* For this two-dimensional mesophase, the alignment by quartz plates also results in a two-dimensional array of

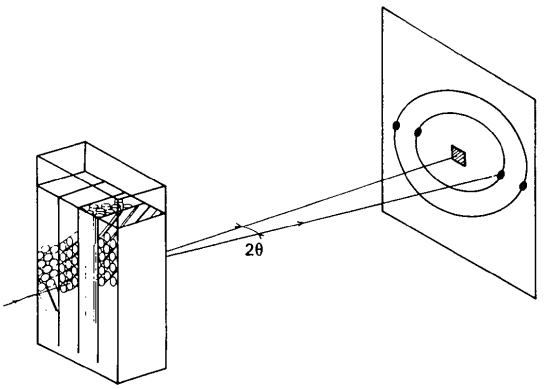

Fig. 3. Scattering geometry for cylinders or ribbons oriented along quartz plates, with the beam parallel to the plates. The rings on the detector are produced by domains where the cyclinders have their long axes parallel to the beam, assuming that these domains can take any orientation about these long axes (see text). The spots on the equatorial line of the detector are produced by domains whose long axis is not along the beam.

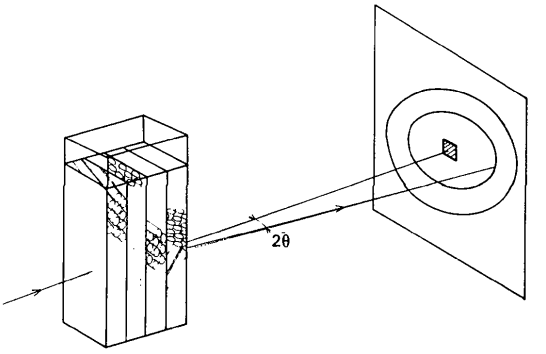

Fig. 4. Scattering geometry for cylinders or ribbons oriented along quartz plates, with the beam normal to the plates. Each domain produces a set of diffraction spots on a line normal to its long axis; the scattering from all domains gives a set of rings with spacings identical to those of a regular powder pattern.

spots, where the incident neutron beam is parallel to the plates; however, this array no longer has exact hexagonal symmetry.

Fig. 7(*a*) shows a diffraction pattern of an intermediate mesophase whose composition is close to the boundary with the hexagonal phase H_α. The geometry is as above, but the detector has been shifted sideways in order to reach higher Q values; thus the center of the beam is located somewhat to the right of the figure. The complete pattern is symmetrical with respect to the vertical axis (mirror symmetry of the sample across the quartz plates) and with respect to the horizontal axis (equator of reciprocal space). Consequently, it is sufficient to consider the upper left quarter of the pattern. It contains the following features:

(i) A set of spots along the equator. As explained in §3.2., most of these spots are produced by all the domains whose long axes are parallel to the plates but not to the beam; because these domains may have different orientations about their long axes, they give a set of spots on the equator which matches all the lines of a powder spectrum.

(ii) A set of spots on a horizontal line parallel to the equator. As explained in §3.2., all these spots must be produced by domains with their long axes parallel to the beam, and a definite orientation within the plane normal to this axis. As the composition of the mesophase changes from the hexagonal towards the lamellar phase, the weak diffraction spots away from the equator become more distinct, emerging from the rings and indicating a stronger preference of the mesophase for aligning a particular set of reticular planes along the plates. Presumably, the origin of this stronger azimuthal orientation is a deformation of the aggregates, which become more like flat ribbons, and tend to have their wide side along the plates (Fig. 7*b*). The unit cell for the domains whose long axes are parallel to the quartz plates and to the beam is constructed as shown in Fig. 7(*b*). The spot at $Q = 0{\cdot}133$ Å^{-1}, $\theta = 67°$ away from the equator marks the (10) vector of the unit cell, while the other unit vector (01) ends on the equator at $Q = 0{\cdot}167$ Å^{-1}. The parallelogram of the monoclinic

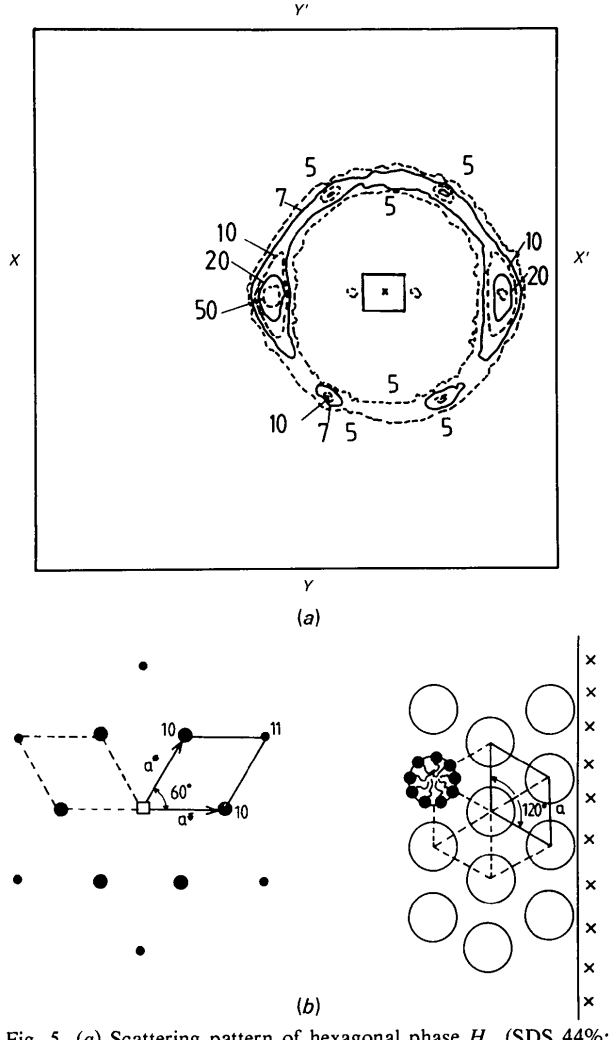

Fig. 5. (*a*) Scattering pattern of hexagonal phase H_α (SDS 44%; D_2O 56% at 328 K) oriented by vertical quartz plates according to the geometry of Fig. 3. The contour map shows two intense peaks and four weak ones on a ring located at 0·131 Å^{-1} from the beam; these six spots form a regular hexagon which is the diffraction pattern for a domain oriented as shown in (*b*). Those domains whose long axes are along the beam contribute equally to the six spots; the other ones scatter only on the two spots which are on the horizontal axis. (*b*) Preferential anchoring of the hexagonal phase cylinders on the quartz plates (right) and the corresponding reciprocal space (left).

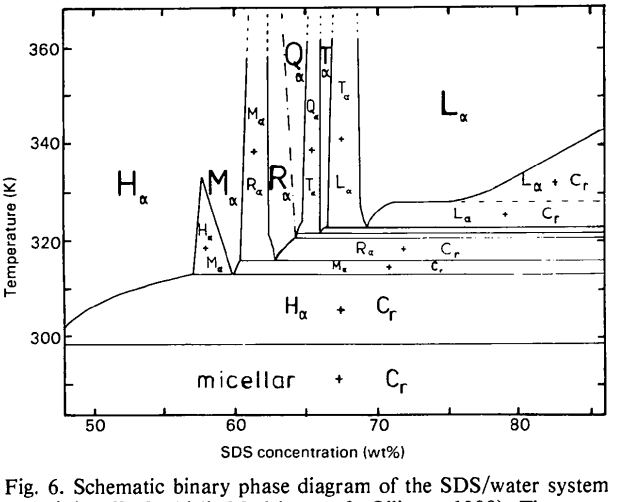

Fig. 6. Schematic binary phase diagram of the SDS/water system (Kékicheff, Grabielle-Madelmont & Ollivon, 1988). The compositions are expressed as a weight percentage of SDS and deuterated water. The boundaries indicated by broken lines are tentative. Luzzati's terminology (Luzzati, 1968) was adopted for the mesophases (the subscript α refers to a quasi-liquid state for paraffinic chains): they are labeled according to the symmetry of their lattice: H_α, hexagonal phase; M_α, two-dimensional monoclinic phase; R_α, rhombohedral phase; Q_α, cubic phase; T_α, tetragonal phase; L_α, lamellar phase. The SDS crystalline hydrates are labeled as Cr.

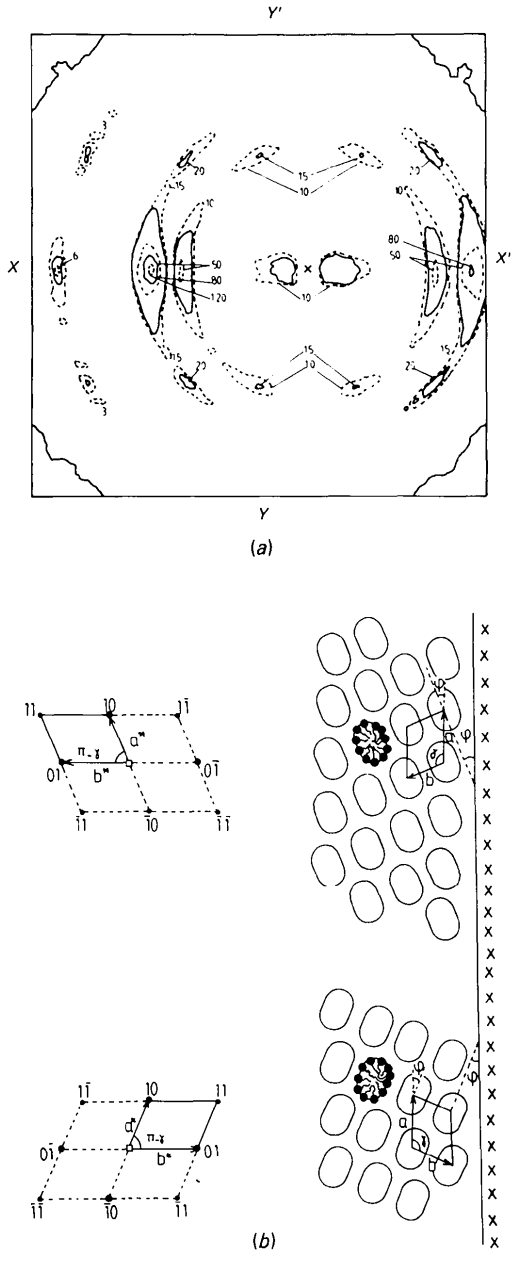

Fig. 7. Diffraction pattern from a sample in the two-dimensional monoclinic phase M_α (SDS 58·5%; $T = 328$ K). The sample is aligned by vertical quartz plates, and the beam is parallel to the plates (see Fig. 3). (*a*) Contour map of the diffraction pattern. The spots away from the equator correspond to two sets of domains, labeled α and β, with their long axes parallel to the beam [see (*b*)]. The crescents on the equator are produced by all domains regardless of the orientation of their long axes with respect to the beam (label γ). (*b*) Unit cells for domains α and β. The resulting assignment of spots in (*a*) is as follows. Horizontal line above the equator, from left to right: 11 (α) $1\bar{1}$ (β), 10 (α), 10 (β), $1\bar{1}$ (α). On the equator, from left to right: 11 (γ), then a double spot containing 01 (α) and $1\bar{1}$ (γ) which is stronger and at smaller Q, then 10 (γ), then the beam-stop surrounded by specular reflexions from the glass plates, then again 10 (γ), $1\bar{1}$ (γ) and 01 (β). The right-hand side of the figure shows the real-space picture of the domains anchored on a quartz plate.

unit cell is completed with the line at $Q = 0{\cdot}251$ Å^{-1}, $\theta = 29°$ indexed as (11). The line at $Q = 0{\cdot}168$ Å^{-1}, $\theta = 46°$ belongs to another set of domains, oriented symmetrically across the vertical plates (Fig. 7*b*); it is indexed as $(1\bar{1})$.

Assuming that there is a single SDS aggregate per unit cell, we can calculate the area of its cross section, because we know the area of the unit cell in real space, and the composition of the mesophase. This yields an area of 1260 Å^2, which could be represented as a rectangle of 42 × 30 Å if the double-layer thickness is kept intermediate between its values in the H_α and L_α phases. If these aggregates were aligned along the long edge of the unit cell in real space, and therefore along the quartz plates, then their edge-to-edge distance would be 9·3 Å and their face-to-face distance 7·6 Å. This last value is quite small, especially when compared with the water-layer thicknesses of lamellar phases (12 Å for the most hydrated one; 7 Å for the least hydrated one). It is more likely that the aggregates make a slight angle (23°) with the unit cell, bringing their face-to-face distance to 11 Å and their edge-to-edge distance to 13 Å. This would also imply that their faces are not exactly parallel to the quartz plates.

3.3.2. *Three-dimensional rhombohedral 'R_α' and cubic 'Q_α' phases.* These two phases are related: the three-dimensional rhombohedral phase R_α can be interpreted as a deformation of the cubic phase Q_α (Kékicheff & Cabane, 1987); therefore we shall discuss them together.

The diffraction patterns from these phases are quite different from those produced by the previous two-dimensional phases. Indeed in the previous phases, all diffraction spots which are located above or below the equator also show up on the equator as explained above; this is caused by a partial (hindered) rotation of the domains about their long axes. Here this effect is absent: we observe a large number of spots away from the equator including some very intense ones on the meridian; none of them have relatives along the equator; conversely the two very intense spots which lie on the equator have no relatives elsewhere in the detector plane. Hence the rotation about an axis parallel to the plates must have ceased; this is in agreement with the symmetries of these phases, which are three-dimensional according to our X-ray results (Kékicheff & Cabane, 1987).

Another remarkable feature is that the spots away from the equator seem to be arranged in vertical bands, which are repeated periodically. This is the type of diffraction pattern which is expected for a rotating single crystal. It is obviously produced by the orientation along the quartz plates, which forces all the domains to rotate around the same crystallographic axis.

In the experimental geometry of Fig. 3, where the beam is parallel to the quartz plates, the samples in the

intermediate rhombohedral R_α or cubic Q_α phases give roughly the same kind of diffraction pattern.* The diffraction pattern shown in Fig. 8(*a*) is obtained from a sample with cubic symmetry. The indexing of the pattern is interpreted in Fig. 8(*b*):

(i) The crystallites turn along the horizontal axis normal to the quartz plates; this axis is the row [111] of the cubic cell.

(ii) The spots are distributed along nearly vertical bands: these bands have a period $\frac{1}{3}|\mathbf{Q}(222)|$.

(iii) The spot 222 on the rotating axis [111] must be produced by domains which are disoriented by at least 17°.

(iv) The relative intensities of the observed spots indicate that the distribution of the crystallites along the row [111] is roughly equiprobable. Indeed these intensities depend on the number of equivalent reflexions which contribute to the same spot in a rotating crystal experiment; for instance the intensity of the Bragg diffraction line at $|\mathbf{Q}| = 0{\cdot}0776$ Å^{-1} ($h^2 + k^2 + l^2 = 2$) is twice as strong in band '0' (contribution from six spots: $10\bar{1}$, $1\bar{1}0$, $0\bar{1}1$, $\bar{1}01$, $\bar{1}10$, $01\bar{1}$) as compared to that in bands '$+\frac{1}{3}$' (contribution from three spots: $\bar{1}\bar{1}0$, $\bar{1}0\bar{1}$, $0\bar{1}\bar{1}$) or '$-\frac{1}{3}$' (contribution from three spots: 110, 101, 011).

Remarkably the distance of the Bragg diffraction spot 222 of the cubic phase Q_α matches periodicity of the lamellar phase L_α ($Q = 0{\cdot}187$ Å^{-1}). Its location on the equator indicates that it corresponds to planes which are parallel to the quartz plates. These planes are normal to the great diagonal [111] of the b.c.c. cell. Hence the shaded planes in Fig. 8(*b*) are features which are akin to the lamellar structure; presumably they contain regions which are locally lamellar and spaced with the same period.

3.3.3. *Three-dimensional tetragonal phase 'T_α'.* Because this phase is limited to a narrow range of concentrations, it is difficult to prepare samples whose composition falls within it. Raising the temperature from 328 to 343 K broadens this concentration range from 0·5 to 1% (Kékicheff, Grabielle-Madelmont & Ollivon, 1988). The pattern shown in Fig. 9 was obtained at 343 K with a sample containing 65·7% SDS, which falls right within the tetragonal phase T_α.

When such samples are obtained, they show a fairly simple diffraction pattern, containing few Bragg diffraction spots (Fig. 9). The profiles are rather odd: they are elongated in a nearly radial direction. This shape could be that of Kossel lines (Guinier, 1956), generated by the large crystallites of the tetragonal phase T_α [indeed, the powder diffraction patterns of the T_α phase consist of many small spots, indicating that the crystallites are much larger than in any of the other mesophases, see Kékicheff & Cabane (1987)]. An alternative interpretation would require a very peculiar misalignment of the crystallites (Rançon & Charvolin, 1988).

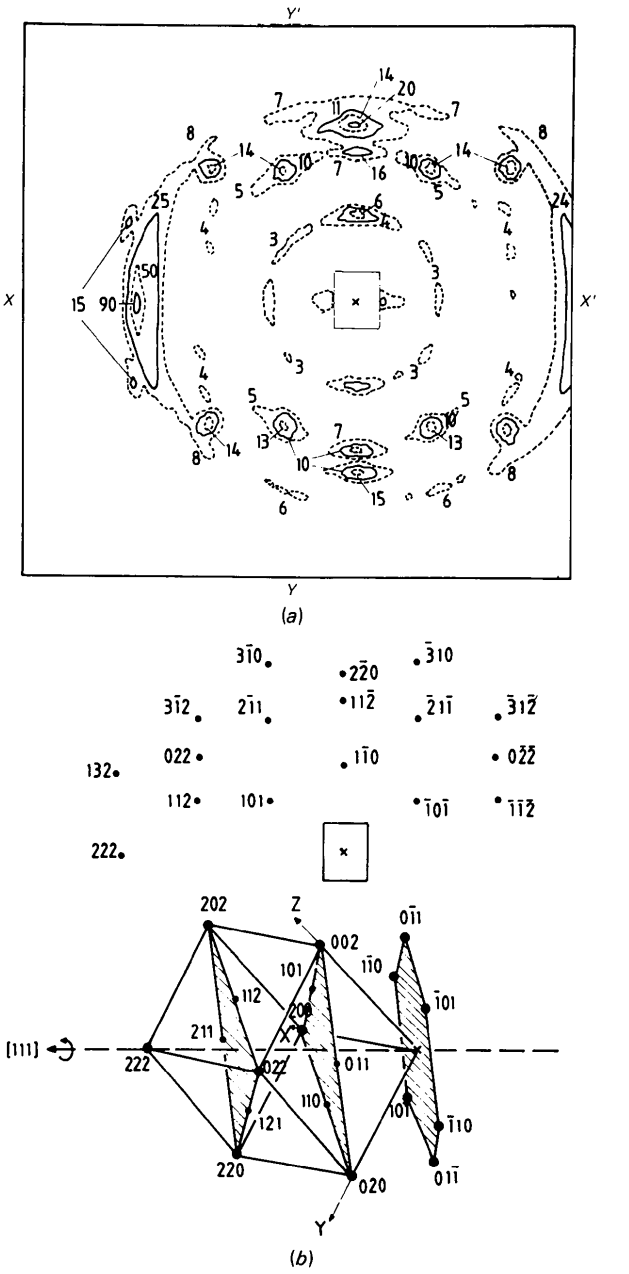

Fig. 8. Diffraction from a sample in the cubic mesophase Q_α (SDS 64%; $T = 328$ K). (*a*) Contour map of the diffraction pattern: the diffraction spots are distributed in vertical bands, which are repeated periodically. This pattern is produced by domains which rotate around the horizontal axis (equator); in the cubic structure this axis is the great diagonal of the cube [111]. (*b*) Unit cell of reciprocal space for a body-centered cubic cell which would produce the diffraction pattern observed in (*a*); the top of the figure shows the locations of the diffraction spots at the same scale as the diffraction pattern in (*a*).

* We recall that through most of the rhombohedral phase, the variation of the unit-cell parameters is very small: the edge length a and the angle α keep values close to those of the cubic phase ($a = 101$ Å; $\alpha = 109{\cdot}48°$) except in a very narrow region close to the highest hydrated boundary of the rhombohedral phase, where the variation is $\leq 10\%$.

The whole pattern is dominated by the strong diffraction at $Q = 0{\cdot}183$ Å^{-1} on the equator. A comparison with the powder diffraction patterns (Kékicheff & Cabane, 1987) indicates that this spot is the 002 diffraction of the tetragonal structure, corresponding to the distance between the square faces of the unit cell. Therefore the unit cell is aligned with its square faces along the quartz plates.

Remarkably, the location of this spot matches that of the first diffraction order of the lamellar phase L_α, suggesting a relation between the bilayers and the square faces of the tetragonal cell. It also matches almost exactly that of the 222 diffraction in the cubic phase Q_α, suggesting another relation between these square faces and some planes of the cubic cell (Fig. 8*b*).

However, the emergence of other spots located away from the equator at $Q = 0{\cdot}127$ Å^{-1}, $\theta = 60°$ with Miller indices 101 (or $\bar{1}01$, ...); $Q = 0{\cdot}161$ Å^{-1}, $\theta = 42°$ (indices 200, or ...) and $Q \simeq 0{\cdot}32$ Å^{-1}, $\theta = 22°$ (indices 400, or 040, ...) suggest that the observed diffraction pattern cannot be produced by a unique orientation of domains. The location of these spots is reproducible; moreover the fact that we observe many discrete orientations for the crystallites is certainly tied to the very large size of these crystallites. Unfortunately, we would have to know the shapes of the aggregates beforehand to explain why these odd orientations are obtained.

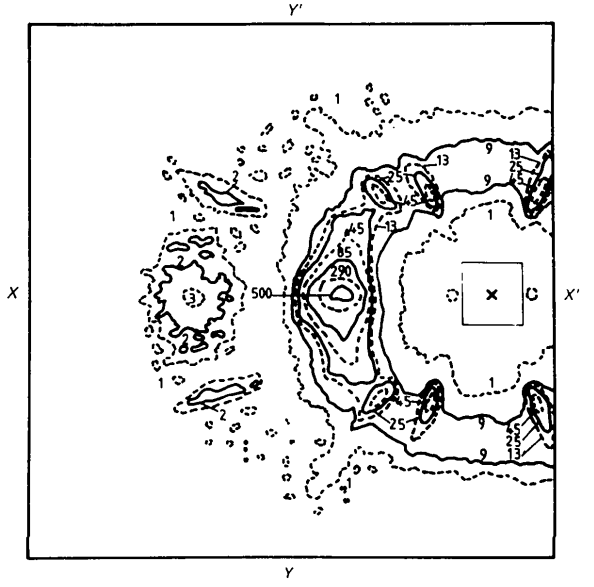

Fig. 9. Diffraction from a sample in the tetragonal mesophase T_α (SDS 65·7%; $T = 343$ K). The strong diffraction on the equator (indexed as 002) matches the 222 spot in the cubic phase Q_α (see Fig. 8*a*) and also the first diffraction order of the lamellar phase L_α (see Fig. 10). The spots observed out the equator result from misaligned domains. They are located in nearly horizontal bands and correspond to Miller indices 400, 200, 101 and again 101 (from left to right). The radially elongated profiles of the Bragg diffraction spots could be generated by the large crystallites of the T_α phase (Kossel lines).

3.4. *Lamellar mesophase 'L_α'*

Fig. 10 shows the diffraction patterns obtained from a lamellar phase L_α oriented by the quartz plates, in the geometry of Fig. 3. The sample composition (69·5% SDS) is close to the most hydrated boundary of the lamellar phase L_α (Fig. 6). The evolution with temperature is shown in Figs. 10(*a–c*). The initial temperature of 326 K is only 3 K above the eutectoid temperature of the lamellar phase L_α (Kékicheff, Grabielle-Madelmont & Ollivon, 1988), and the temperature rise up to 343 K follows a vertical line in the vicinity of the boundary to the previous phase T_α (Fig. 6).

All these diffraction patterns are dominated by the strong diffraction at $Q \simeq 0{\cdot}18$ Å^{-1} on the horizontal axis. This diffraction corresponds to the first diffraction order of the layers ($d = 2\pi/Q = 33$ Å). The location of these spots on the horizontal axis indicates that the layers are aligned parallel to the quartz plates; because the lamellar phase is uniaxial, its reciprocal space must have a symmetry of revolution around the normal to the layers, which is here the horizontal axis. In addition, the lamellar phase of SDS/water also shows some additional regions of diffuse scattering at small angles, which would not occur for flat bilayers (Kékicheff, Cabane & Rawiso, 1984*b*). The features of this diffuse scattering and their evolution with temperature (which is completely reversible) are remarkable:

(i) At 'low' temperature (326 K), the diffraction pattern shown in Fig. 10(*a*) indicates that the diffuse scattering is concentrated in small spots. Their locations are in the vicinity of the Bragg spots of the tetragonal phase T_α (Fig. 9). However, they are not produced by a small amount of T_α phase in the sample; indeed their widths are now much broader than the resolution of the experiment and consequently larger than the tetragonal Bragg spots.

(ii) When the temperature of the lamellar phase L_α is increased (333 K), the region of diffuse scattering broadens considerably (Fig. 10*b*) and the spots progressively merge into diffuse stripes (343 K; Fig. 10*c*).

(iii) At still higher temperatures (348 K), these stripes become thicker and longer (Kékicheff, Cabane & Rawiso, 1984*b*).

As discussed in our previous work (Kékicheff, Cabane & Rawiso, 1984*b*), these stripes are the section of a cylinder whose axis is normal to the bilayers (horizontal axis in Fig. 10); because this cylinder is elongated in the direction normal to the bilayers, it corresponds to defects whose correlations extend only within one bilayer but not between consecutive bilayers. At lower temperatures (below 333 K) the stripes

become modulated in the direction normal to the bilayers: then the region of diffuse scattering consists of four rings around the axis of symmetry; these rings correspond to interlayer correlations whose periods match those of the T_α phase (*cf.* Fig. 9).

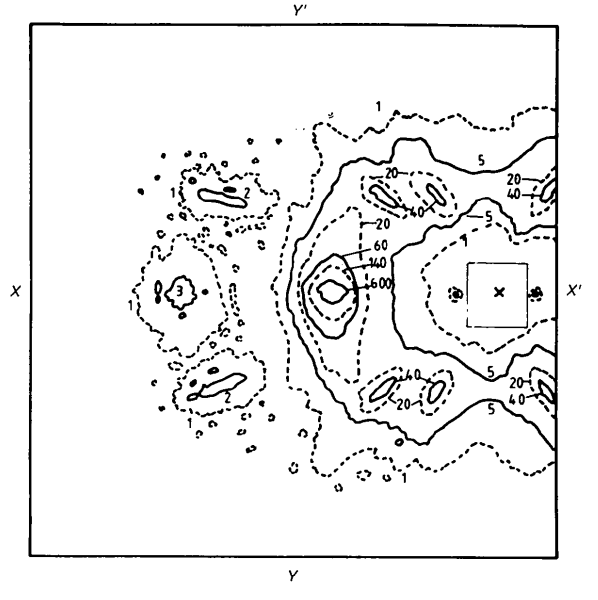

(*a*)

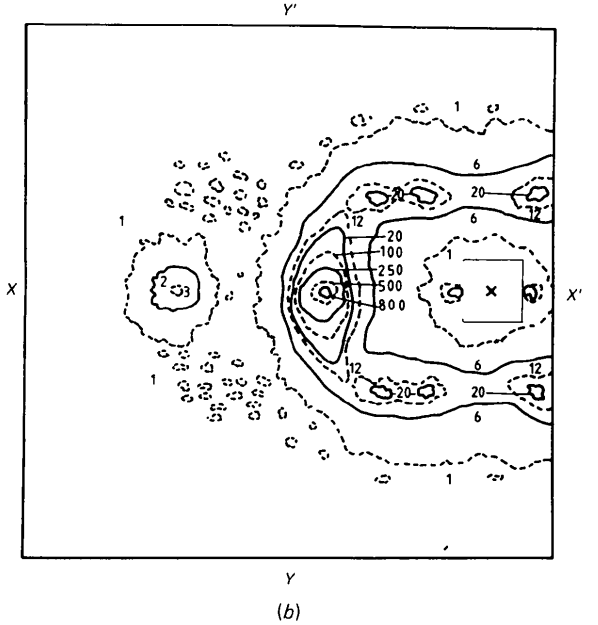

(*b*)

Fig. 10. Diffraction patterns obtained from a sample in the lamellar phase L_α (SDS 69·5%) near the boundary to the tetragonal phase T_α (see Fig. 6). All these diffraction patterns are dominated by the first diffraction order located on the equator. The spots or bands from the equator are produced by defects in the bilayers, which become organized as the temperature is raised: (*a*) $T = 326$ K, (*b*) 333 K.

4. Discussion

4.1. *Leading crystallographic planes*

Our aim is to determine the shapes of the amphiphilic aggregates and the way in which they are stacked in the structure. The information which we have obtained previously (Kékicheff & Cabane, 1987) does not fulfill this aim: from powder diffraction experiments we have determined the symmetry of the unit cell of each phase but not its content. Moreover, the classical method where this content is obtained from the relative intensities cannot be used, because the form factor of an SDS aggregate is not simple: polar heads and aliphatic tails have scattering densities on either side of water (Luzzati, 1968). Here the use of oriented samples brings additional information: indeed the mesophases tend to align their leading crystallographic planes along the quartz plates; therefore these planes can be identified.

The case of the lamellar phase L_α is trivial (bilayers parallel to the quartz plates), but the transition from a one-dimensional to a three-dimensional phase is rather illuminating in this respect. Indeed the strong Bragg diffraction of the lamellar phase L_α is retained in the adjacent tetragonal phase T_α [**Q**(002)] and cubic phase Q_α [**Q**(222)], with the same modulus and the same direction with respect to aligning the quartz plates. Therefore, the structures of these three-dimensional phases contain some reticular planes which are locally lamellar, and which are capable of anchoring along the quartz planes. For the tetragonal phase T_α, these pseudo-lamellar planes correspond to the square faces

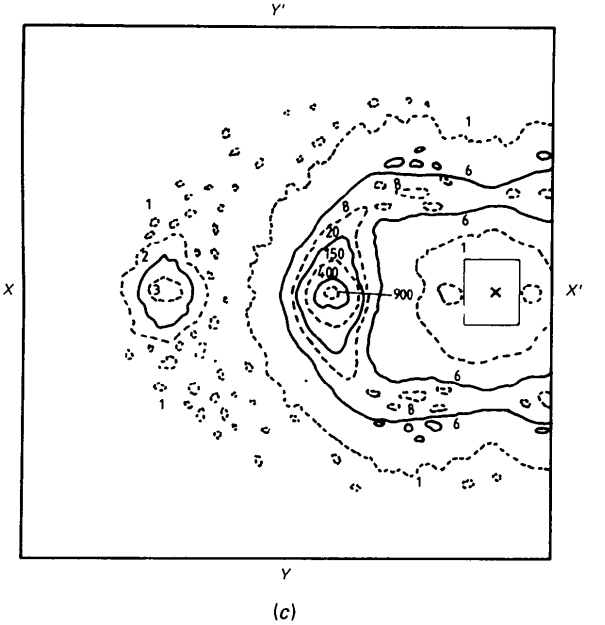

(*c*)

Fig. 10 (*cont.*). Diffraction patterns obtained from a sample in the lamellar phase L_α: (*c*) $T = 343$ K.

of the unit cell; they are made of rods which meet orthogonally at the vertices and these square lattices of rods are staggered on top of each other in the unit cell (Luzzati, Tardieu & Gulik-Krzywicki, 1968). For the cubic phase Q_α the pseudo-lamellar planes correspond to the shaded areas in Fig. 8(*b*); here the analysis is more delicate, since the edges of the cubic cell are not along these planes. A likely hypothesis would be that the edges of the unit cell define the axes of a set of 'rods' which are joined at the vertices. It is the outer surfaces of these rods which form the pseudo-lamellar planes; a structure of this type has been presented by Siegel (1986). However this is not the only way in which a lamellar structure can be built from a cubic one (Rançon & Charvolin, 1987, 1988).

The case of the two-dimensional phases (hexagonal H_α and monoclinic M_α) is also interesting because it illustrates the nature of these 'leading' crystallographic planes. Indeed the reticular planes of the hexagonal phase H_α which are anchored along the quartz plates are the planes where the cylinders are closest to each other: they are the (10) planes and not the (11), where the repetition of the cylinders would be $\sqrt{3}$ times longer. Thus the planes which are anchored are the densest planes of the structure; they are also the planes along which the structure can be sheared easily.

In the monoclinic phase M_α, the longest edge of the unit cell is aligned along the quartz plates (Fig. 7*b*). Here as well, this alignment brings the densest reticular planes close to the quartz plates; indeed the planes which are parallel to the ribbon's faces are less dense because the ribbons are packed in a staggered configuration. This choice of reticular planes for anchoring is analogous to that of the hexagonal phase H_α.

4.2. *Dimensions of the aggregates*

Is it sufficient to identify these leading crystallographic planes in order to reconstruct the structure in real space? The best case would be the cubic phase, where we would have four sets of 'dense' planes, each normal to one of the cube's great diagonals; the intersection of these four sets of planes might define the shapes of the interfaces to a good approximation.

The situation is less favorable in the structures which only contain one set of 'dense' planes, such as the ribbon phase M_α, or the T_α and L_α phases. Here we must try to build objects which are essentially parallel to these planes but which are limited by the dimensions of the unit cell. In the tetragonal phase T_α, the shape of the unit cell and its relation to the cubic structure suggest that the basic element could be a flat lattice of orthogonal rods; in one such lattice the rods would be along the edges of the unit cell's square center of the unit cell.

A 'trace' of this structure may exist in the neighboring lamellar phase L_α, as evidenced by the diffuse scattering which is discussed in §4.3. In this sense the unit cell would remain finite, and would be described as a piece of bilayer which would be corrugated in a fashion similar to the lattices of the T_α phase.

In the monoclinic phase M_α we already know that the aggregates are ribbons (*i.e.*, deformed cylinders) whose thickness (~28 Å) and width (~40 Å) are largely determined by the dimensions of the unit cell and by the packing constraints. The problem lies with the third dimension of the unit cell, which in a true two-dimensional phase would be infinite. Here the use of oriented samples reveals a feature which was not obvious in the powder diffraction spectra (Kékicheff & Cabane, 1987): there is a broad band of diffuse scattering which runs parallel to the equator and has a sharp inner edge at $Q_{\min} = 0{\cdot}10$ Å^{-1}. This diffuse scattering may indicate a modulation along the length of the ribbons. Indeed such a modulation would appear in reciprocal space as a set of diffuse planes normal to the ribbon's long axes; since the sample contains many domains with different orientations of their long axes along the quartz plates, the diffuse planes will intersect the vertical plane along horizontal lines which are piled up beyond a minimum Q value which is obtained for ribbons normal to the beam: $Q_{\min} = 0{\cdot}10$ Å^{-1} corresponds to a pseudoperiod of 60 Å for this modulation. This hypothesis will have to be confirmed by experiments on monodomains of the M_α phase.

4.3. *Relations between consecutive structures*

When intermediate mesophases are oriented, their diffraction patterns look surprisingly similar to each other (Figs. 5, 7–10). This is in contrast to their powder spectra, where the different symmetries of the phases yield very different patterns (Kékicheff & Cabane, 1987). This apparent conflict can be resolved as follows: oriented samples give a reciprocal picture of the unit cell, which appears to evolve in a nearly continuous way; powder samples give sets of lines whose packing depends on the symmetries of the phases, and these symmetries do not change in a systematic way. Hence we conclude that the shapes of the aggregates vary nearly continuously throughout the concentration range, whereas the symmetry of their packing cannot evolve in such a continuous way [for a different analysis of a transformation from a hexagonal to a lamellar phase, see Hendrikx & Charvolin (1981), Alpérine, Hendrikx & Charvolin (1985) and Rançon & Charvolin (1987)].

Still, we must rationalize the general direction of this evolution. In amphiphilic systems, the classical argument is based on the curvatures of the interfaces, where it is argued that changes in the relative volumes of the

polar and apolar regions result in a unique value for the curvature of the polar/apolar interfaces (Winsor, 1968). However, the application of this model to intermediate phases is vastly complicated by the fact that the ribbons have inhomogeneous curvatures; therefore, a proper theory must consider not only the mean curvature and the Gaussian curvature, but also their spatial gradients. Moreover, this description ignores the forces between aggregates, which may be just as large as the forces within the aggregates.

Here we shall list two cases where the interplay of intra- and interaggregate forces is rather obvious. The first one is the transition from the two-dimensional monoclinic M_α (or deformed hexagonal) phase to the three-dimensional rhombohedral R_α (or deformed cubic) phase. The M_α phase is made of ribbons; as the concentration of SDS rises, these ribbons become wider and they must rotate in the unit cell in order to avoid each other (Fig. 7*b*). At the transition to the R_α phase we assume that this angle has reached the value of 23° which minimizes this interference between ribbons which are side by side. Further growth of ribbon width is prohibited by repulsion; it may then become more advantageous to accommodate the extra SDS by making connexions between neighboring ribbons; this generates a three-dimensional phase and at this point the distinction between inter- and intraaggregate forces collapses.

The other example concerns the corrugations of the tetragonal T_α and lamellar L_α phases. At high temperature or large SDS concentration, the bilayers of the L_α phase appear to be flat; however, a specific class of defects appears when the temperature is lowered or hydration increased. To some extent this could be interpreted solely in terms of intraaggregate forces, assuming that the large size of the SDS headgroup makes it unfavorable to retain zero curvature.* However, as the boundary to the T_α phase is approached, the defects become correlated from one bilayer to the neighboring one; thus the phase transition extends these correlations into a long-range order which forms the T_α phase: here again the inter- and intra-aggregate forces are comparable in importance, and the distinction between them is not useful.

A proper analysis should take into account all forces at a molecular level. For ionic amphiphiles in water, five forces must be considered. The first is an indirect attraction between apolar groups which are in contact with water; it acts as a surface tension on the hydrocarbon/water interface. Next are the direct electrostatic interactions between all charges located on the polar heads and counterions, and also a hydration force, which results in an indirect repulsion between charges or dipoles separated by water. Then there are entropic forces, corresponding to the mixing of ions with water and to the configurational freedom of the hydrocarbon chains. All these forces are of comparable magnitude, but they change in different directions when the thicknesses or the geometry of the aggregates are changed.

* When the temperature rises, the chains tend to resist the stretching which is imposed on them by the mesophase (rubber elasticity); consequently, their lateral pressure will be larger, and they will oppose the production of a region with positive curvature of the interface. Conversely, when the surfactant concentration is increased at constant temperature, there will be loss of water to hydrate each polar head, and the lateral pressure between head groups will decrease; this effect will also oppose the production of defects with a positive curvature of the interface.

5. Concluding remarks

The SDS/water system crosses from a situation of homogeneously curved interfaces (cylinders) to a situation of flat surfaces (bilayers) through a series of four intermediate mesophases. The symmetries of these mesophases are quite different from each other and from the two extreme phases, yet the reciprocal space observed for oriented samples evolves in a nearly continuous way from one end of the concentration range to the other. The aggregates of amphiphilic molecules which build the structure must change their shapes accordingly. Starting from the least hydrated phase (lamellar), we first observe a periodic corrugation of the bilayers, which is then replaced by a periodic modulation in two directions: the bilayers are turned into flat square lattices of connected rods. The transformation to the neighboring three-dimensional phase may proceed through an interconnection of these lattices, which produces an isotropic cubic structure. Then this array of rods is distorted to form a rhombohedral phase. Subsequently, the connections between the rods are severed: this produces a two-dimensional array of anisotropic ribbons which may still be modulated along their long axes. The last step is the transition to a system of circular cylinders which occurs partly at the transition to the hexagonal phase and partly through the composition range of the hexagonal phase.

It is a pleasure for us to thank M. Rawiso and M. Roth for their assistance and advice in the neutron-scattering experiments performed at ILL in Grenoble. We gratefully acknowledge the material help and advice from staff members of LLB and ILL including A. Brulet, M. Cruz and B. Farnoux.

References

ALPÉRINE, S., HENDRIKX, Y. & CHARVOLIN, J. (1985). *J. Phys. (Paris) Lett.* **46**, L27–L31.

CHARVOLIN, J. & SADOC, J. F. (1987). *J. Phys. (Paris)*, **48**, 1559–1569.

CHARVOLIN, J. & TARDIEU, A. (1978). *Solid State Physics*, Vol. 14, edited by F. SEITZ & D. TURNBULL, p. 209. New York: Academic Press.
EKWALL, P. (1975). *Advances in Liquid Crystals*, Vol. 1, edited by G. H. BROWN, ch. 1, p. 1. New York: Academic Press.
GUINIER, A. (1956). *Théorie et Technique de la Radiocristallographie*. Paris: Dunod.
HENDRIKX, Y. & CHARVOLIN, J. (1981). *J. Phys. (Paris)*, **42**, 1427–1440.
HENDRIKX, Y., CHARVOLIN, J., KÉKICHEFF, P. & ROTH, M. (1987). *Liq. Cryst.* **2**(5), 677–687.
KÉKICHEFF, P. & CABANE, B. (1987). *J. Phys. (Paris)*, **48**, 1571–1583.
KÉKICHEFF, P., CABANE, B. & RAWISO, M. (1984*a*). *J. Colloid Interface Sci.* **102**, 51–72.
KÉKICHEFF, P., CABANE, B. & RAWISO, M. (1984*b*). *J. Phys. (Paris) Lett.* **45**, L813–L821.
KÉKICHEFF, P., GRABIELLE-MADELMONT, C. & OLLIVON, M. (1988). *J. Colloid Interface Sci.* In the press.
LUZZATI, V. (1968). *Biological Membranes*, Vol. 1, edited by D. CHAPMAN, ch. 3, pp. 71–123. New York: Academic Press.
LUZZATI, V., TARDIEU, A. & GULIK-KRZYWICKI, T. (1968). *Nature (London)*, **217**, 1028–1030.
RANÇON, Y. & CHARVOLIN, J. (1987). *J. Phys. (Paris)*, **48**, 1067–1073.
RANÇON, Y. & CHARVOLIN, J. (1988). *J. Chem. Phys.* Submitted.
SADOC, J. F. & CHARVOLIN, J. (1986). *J. Phys. (Paris)*, **47**, 683–691.
SIEGEL, D. P. (1986). *Chem. Phys. Lipids*, **42**, 279–292.
WINSOR, P. A. (1968). *Chem. Rev.* **68**, 1–40.

Acta Cryst. (1988). B**44**, 406–412

Structural Studies of Analgesics and Their Interactions. XII. Structure and Interactions of Anti-inflammatory Fenamates. A Concerted Crystallographic and Theoretical Conformational Study

BY V. DHANARAJ AND M. VIJAYAN

Molecular Biophysics Unit, Indian Institute of Science, Bangalore-560012, *India*

(*Received* 21 *September* 1987; *accepted* 25 *January* 1988)

Abstract

A theoretical conformational analysis of fenamates, which are *N*-arylated derivatives of anthranilic acid or 2-aminonicotinic acid with different substituents on the aryl (phenyl) group, is reported. The analysis of these analgesics, which are believed to act through the inhibition of prostaglandin biosynthesis, was carried out using semi-empirical potential functions. The results and available crystallographic observations have been critically examined in terms of their relevance to drug action. Crystallographic studies of these drugs and their complexes have revealed that the fenamate molecules share a striking invariant feature, namely, the six-membered ring bearing the carboxyl group is coplanar with the carboxyl group and the bridging imino group, the coplanarity being stabilized by resonance interactions and an internal hydrogen bond between the imino and carboxyl groups. The results of the theoretical analysis provide a conformational rationale for the observed invariant coplanarity. The second six-membered ring, which provides hydrophobicity in a substantial part of the molecule, has limited conformational flexibility in meclofenamic, mefenamic and flufenamic acids. Comparison of the conformational energy maps of these acids shows that they could all assume the same conformation when bound to the relevant enzyme. The present study provides a structural explanation for the difference in the activity of niflumic acid, which can assume a conformation in which the whole molecule is nearly planar. The main role of the carboxyl group appears to be to provide a site for intermolecular interactions in addition to helping in stabilizing the invariant coplanar feature and providing hydrophilicity at one end of the molecule. The fenamates thus provide a good example of conformation-dependent molecular asymmetry.

Introduction

Fenamates are a family of potent anti-inflammatory analgesics, prominent among them being meclofenamic, mefenamic, flufenamic and niflumic acids (Fig. 1). All of them, except niflumic acid (2-{[3-(trifluoromethyl)phenyl]amino}-3-pyridinecarboxylic acid), are *N*-aryl-substituted derivatives of anthranilic acid. The therapeutic activity of these analgesics is believed to be due to their ability to inhibit the biosynthesis of prostaglandins (Flower, 1974). In order to elucidate the mechanism by which they exert their influence on the enzymatic system, it is essential to have a thorough understanding of their molecular geometry, the interactions they are likely to be involved in, and the consequences of these interactions on their electronic structure and molecular geometry. An ongoing project in our laboratory, which was earlier concerned with anti-inflammatory pyrazole derivatives (Singh & Vijayan, 1974, 1977; Krishna Murthy, Vijayan & Brehm, 1979; Krishna Murthy & Vijayan, 1981*a*; Vijayan,

0108-7681/88/040406-07$03.00